Investigation of ab Initio HF-SCF-CI Methods for Calculating Rotatory Strengths in (*R*)-3-Methylcyclobutene

C. F. Chabalowski,[†] G. M. Maggiora, and R. E. Christoffersen*[‡]

Contribution from the Department of Chemistry, University of Kansas, Lawrence, Kansas 66045.
Received July 23, 1984

Abstract: As a prototype study designed to assess the possibility of calculating ab initio rotatory strengths in large molecular systems, configuration interaction (CI) wave functions have been determined and subsequently used to calculate the rotatory strengths for several low-lying singlet–singlet transitions in (*R*)-3-methylcyclobutene. Special attention is given to the $^1(\pi \rightarrow \pi^*)$ transition, and six basis sets are used which range in quality from less-than-single-ζ to double-ζ-plus diffuse (DZD) functions. The sign of the rotatory strength associated with the $^1(\pi \rightarrow \pi^*)$ excitation is shown to be independent in this molecule of the basis set, although substantial flexibility is needed in order to describe the $^1(\pi,\pi^*)$ state accurately. When the calculated results are used and comparison is made to other molecules, a different assignment of the circular dichroism spectra from that reported earlier is suggested. Strong similarities are seen between the states calculated here by using the DZD basis and the low-lying singlet states in ethylene. An examination of transition dipole moment matrix elements over configurations also shows a sensitivity of the calculated rotatory strength to both large and small CI contributors. This implies the need to determine a relatively flexible CI wave function and to use all terms in order to assure reliable rotatory strengths.

I. Introduction

While ab initio quantum mechanical studies of ground states, both from a geometric and electronic structural point of view, have been applied to a broad range of molecules, substantially less emphasis has been placed upon application of these techniques to spectral problems. In particular, use of ab initio techniques to understand and predict optical rotatory dispersion/circular dichroism (ORD/CD) spectra of large molecules has had few applications. Since a wide variety of ab initio approaches is possible, it is appropriate to elucidate the characteristics that would be desirable in a method if it is to be useable in general.

The purpose of this study is to investigate the applicability of ab initio self-consistent-field (SCF) and configuration interaction (CI) methods in the calculation of CD spectra in organic molecules. The primary emphasis is to explore the stability of the calculated rotatory strengths with respect to the ab initio approach and basis set used. Specifically, the rotatory strengths of low-lying electronic transitions in (*R*)-3-methylcyclobutene (3MCB) (see Figure 1) are investigated by using different-sized basis sets and the CI configuration generation scheme developed by Whitten and Hackmeyer.[1]

Particular attention is given to the lowest $^1(\pi \rightarrow \pi^*)$ transition, which was assigned a negative rotatory strength in earlier studies.[2] However, later experimental and theoretical work[3] raised questions as to whether this negative CD peak belongs to the $^1(\pi \rightarrow \pi^*)$ or to the Rydberg ($\pi \rightarrow$ 3s) transition. Specifically, studies of the absorption and CD spectra of (*R*)-3-methylcyclopentene (3MCP), which differs from 3MCB by an additional ring carbon, indicate a positive sign for the CD band, corresponding to the $S(\pi,\pi^*) \leftarrow S_0$ transition.

Reasons for choosing 3MCB as a model olefin include the following: (1) it possesses a relatively rigid ring with no large groups or side chains whose orientation might be difficult to determine; (2) it is small enough to treat within an ab initio framework and still use a variety of basis sets; and (3) experimental data are available for direct comparison with calculated results. Another aspect of interest in this molecule is that the methyl group gives rise to the CD spectrum, because of its asymmetric perturbation of an otherwise inherently symmetric chromophore. Usual prototype theoretical studies of optical activity in monoolefins involve calculations on twisted ethylene, which is an example of a nonexperimentally accessible asymmetric chiral molecule.[4-7] Regardless of the cause of the chirality, many similarities between the low-lying electronic states in ethylene and other monoolefins have been established and are noted below for use in the current study.

II. Ethylene Studies

Theoretical and experimental evidence indicates that the lowest lying singlet transition in ethylene, and in most larger monoolefins, is to a Rydberg $S_1(\pi,3s)$ state.[8-15] The next state is also assigned as a Rydberg state. In ethylene it is represented as a transition of a π electron into a 3p antibonding orbital, which lies in a CH_2 plane of the molecule.[12,15-19] This transition to the $S_2(\pi,3p)$ state would be electric dipole forbidden in planar ethylene but becomes allowed as ethylene is twisted about its C–C bond.

[†]Current address: Abbott Laboratories, Department 47E, Abbott Park, North Chicago, IL 60064.
[‡]Current address: Th Upjohn Company, Kalamazoo, MI 49001.

(1) Whitten, J. L.; Hackmeyer, M. *J. Chem. Phys.* **1969**, *51*, 5584–5596.
(2) Rossi, R.; Diversi, P. *Tetrahedron* **1970**, *26*, 5033–5039.
(3) Levi, M.; Cohen, D.; Schurig, V.; Basch, H.; Gedanken, A. *J. Am. Chem. Soc.* **1980**, *102*, 6972–6975.
(4) Bouman, T. D.; Hansen, A. E. *J. Chem. Phys.* **1977**, *66*, 3460–3467. See also: Robin, M. B.; Basch, H.; Kuebler, N. A.; Kaplan, B. E.; Meinwald, J. *J. Chem. Phys.* **1968**, *48*, 5037–5047.
(5) Rauk, A.; Jarvie, J. O.; Ichimura, H.; Barriel, J. M. *J. Am. Chem. Soc.* **1975**, *97*, 5656–5664.
(6) Liskow, D. H.; Segal, G. A. *J. Am. Chem. Soc.* **1978**, *100*, 2945–2949.
(7) For a recent example of an ab initio configuration study on an experimentally accessible system, see: Segal, G. A.; Wolf, K.; Diamond, J. J. *J. Am. Chem. Soc.* **1984**, *106*, 3175–3179.
(8) Loeffler, B. B.; Eberlin, E.; Pickett, L. *J. Chem. Phys.* **1958**, *28*, 345–347.
(9) Carr, E. P.; Stücklen, H. *J. Chem. Phys.* **1936**, *4*, 760–768.
(10) Robin, M. B.; Keubler, N. A. *J. Mol. Spectrosc.* **1970**, *33*, 274–291.
(11) Katz, B.; Jortner, J. *Chem. Phys. Lett.* **1968**, *2*, 437–439.
(12) McMurchie, L. E.; Davidson, E. R. *J. Chem. Phys.* **1977**, *66*, 2959–2971.
(13) Buenker, R. J.; Peyerimhoff, S. D. *Chem. Phys.* **1975**, *9*, 75–89.
(14) (a) Price, W. C.; Tutte, W. T. *Proc. R. Soc. London, Ser. A* **1940**, *A174*, 207–220. (b) Wilkinson, P. G.; Mulliken, R. S. *J. Chem. Phys.* **1955**, *23*, 1895–1909. (c) Wilkinson, P. G. *Can. J. Phys.* **1956**, *34*, 643–652.
(15) Buenker, R. J.; Peyerimhoff, S. D.; Kammer, W. E. *J. Chem. Phys.* **1971**, *55*, 814–827.
(16) Mulliken, R. S. *J. Am. Chem. Soc.* **1964**, *86*, 3183–3197.
(17) Fischbach, U.; Buenker, R. J.; Peyerimhoff, S. D. *Chem. Phys.* **1974**, *5*, 265–276.
(18) Buenker, R. J.; Peyerimhoff, S. D.; Hsu, H. L. *Chem. Phys. Lett.* **1971**, *53*, 65–70.
(19) Peyerimhoff, S. D.; Buenker, R. J. *Theor. Chim. Acta* **1972**, *27*, 243–264.

0002-7863/85/1507-1632$01.50/0

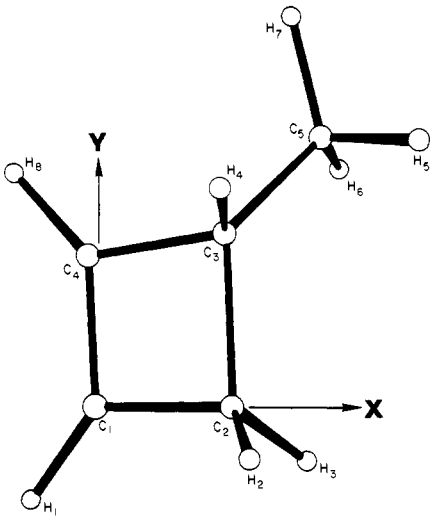

Figure 1. Orientation of 3MCB molecule in coordinate axes. C_1 lies on the origin, the bond between C_1–C_2 defines the positive x axis, and atoms (C_1, C_2, C_3) define the x, y plane for all geometries. A right-handed coordinate system is employed to define the z axis.

An $S_3(\pi,\pi^*)$ state, often called the V state, is reported to have the next highest transition energy, E = 7.65 eV,[14b] lying very close in energy to the aforementioned $S_2(\pi,3p)$ state. Much work has gone into determining whether this state is a valence or Rydberg state or perhaps a state of intermittent diffuseness. Experimental evidence appears to indicate that the $S_3(\pi,\pi^*)$ state possesses more valence character than would be expected for a Rydberg state.[10,11,20]

Early calculations using basis sets without diffuse basis functions expectedly predicted the $S_3(\pi,\pi^*)$ state as a valence state with an excitation energy substantially above the experimentally observed energy of 7.65 eV. For example, Schulman et al.[21] used such a basis set and calculated the transition energy to be 9.30 eV, with an oscillator strength of 0.74 as compared to an experimental oscillator strength of 0.34. Later, Dunning et al.[22] included s- and p-type diffuse functions and calculated an energy of 8.28 eV for the same transition. Again, the calculated oscillator strength of 0.12 differed considerably from the experimental value. The description of the V state was at that point a diffuse, Rydberg-like state. Buenker and Peyerimhoff[13,15] used a larger basis set including diffuse functions and polarization functions plus an extensive CI and calculated a reasonable transition energy of 8.12 eV and oscillator strength of f = 0.29. However, the $S_3(\pi,\pi^*)$ state was considerably less diffuse than that calculated by Dunning et al.[22] Extensive CI calculations by McMurchie and Davidson,[12] using a basis set similar to that of Buenker and Peyerimhoff,[13] found a transition energy of 7.93 eV with an oscillator strength of f = 0.36. From the second moment for the π^* natural orbital, McMurchie and Davidson concluded that the $S_3(\pi,\pi^*)$ state is relatively valence-like. And most recently, Buenker et al.[23] conclude "that a significant amount of diffuse character is essential for the accurate representation of this electronic wave function". This conclusion was based, in part, on a calculation in which the diffuse d functions were removed, causing a 0.6-eV rise in the $^1(\pi,\pi^*)$ state energy and a calculated oscillator strength larger than the experimentally observed value of f = 0.34. In light of the results of these most recent studies, it seems appropriate to consider the $^1(\pi,\pi^*)$ state as being neither pure valence nor pure Rydberg but rather as a state of intermittent diffuseness.

The current study includes calculation of singlet–singlet transition energies, oscillator strengths, and rotatory strengths for transitions to the three lowest singlet excited states in 3MCB. Particular attention is given to the calculated sign of the rotatory strength for the transition to the $^1(\pi,\pi^*)$ state for five different valence-like basis sets, i.e., basis sets without diffuse basis functions. A sixth basis set, which included diffuse functions, was also tested, and comparison of these results with the results from the valence basis sets gives information as to the sensitivity of the rotatory strength to inclusion of diffuse nature in the description of the $^1(\pi,\pi^*)$ state in 3MCB. Attention is also given to the role that $^1(\sigma,\pi^*)$ states play in these lower energy transitions, since the σ-bond strain in the four-membered ring would be expected to raise the filled σ-molecular orbitals (σ-MO's) relative to the π-MO, thus producing lower energy excitations.[7,24,25]

III. Theory

Ab initio closed-shell self-consistent-field MO calculations are first carried out on the ground state to obtain a set of MO's appropriate for CI calculations. The SCF wave function is determined in the Roothaan–Hall formulation[26] and is written as a single Slater determinant of molecular spin–orbitals (a_i), which for an N-electron molecule is given by

$$\Phi_{[SCF]} = (N!)^{-1/2}|a_1(1)\ a_2(2)...a_N(N)| \tag{1}$$

The CI wave function for the Kth state (Ψ_K) is described as a linear combination of configurations,

$$\Psi_K = \sum_j C_{jK}\Phi_j \tag{2}$$

where each configuration, Φ_j, may be a linear combination of Slater determinants. The procedure for determination of the CI wave function has been given earlier.[1]

The electrical dipole transition moment ($\mu^{K,L}$) between states K and L can be written as

$$\mu^{K,L}(\nabla) = \langle\Psi_K|\mu(\nabla)|\Psi_L\rangle \tag{3}$$

where

$$\mu(\nabla) = \sum_i \nabla_i \tag{4}$$

and is known as the "velocity form" of the transition moment operator. Alternatively, the "length form" of the transition moment operator can be used, i.e.,

$$\mu^{K,L}(r) = \langle\Psi_K|\mu(r)|\Psi_L\rangle \tag{5}$$

where $\mu(r)$ is given by

$$\mu(r) = \sum_i r_i \tag{6}$$

The two forms of $\mu^{K,L}$ represented in eq 3 and 5 are known to be equivalent for the exact electronic wave function,[27] although the velocity form has advantages for approximate wave functions because of its invariance to choice of origin.

The oscillator strength is given by

$$f^{K,L}(\nabla) = \frac{2}{3}(E_L - E_K)^{-1}|\mu^{K,L}(\nabla)|^2 \tag{7}$$

in the velocity form and by

$$f^{K,L}(r) = \frac{2}{3}(E_L - E_K)|\mu^{K,L}(r)|^2 \tag{8}$$

in the length form.

Just as the oscillator strength gives the intensity of an absorption band, the rotatory strength, $R^{K,L}$ gives the intensity of a CD band.

(20) Myron, E.; Raz, B.; Jortner, J. *Chem. Phys. Lett.* **1970**, *6*, 563–565.
(21) Schulman, Jj. M.; Moscowitz, J. W.; Hollister, C. *J. Chem. Phys.* **1967**, *46*, 2759–2764.
(22) Dunning, T. H.; Hunt, W. J.; Goddard, W. A. *Chem. Phys. Lett.* **1969**, *4*, 147–150.
(23) Buenker, R. J.; Shih, S. K.; Peyerimhoff, S. D. *Chem. Phys.* **1979**, *36*, 97–111.
(24) Robin, M. B. "High Excited States of Polyatomic Molecules"; Academic Press: New York, 1975; Vol. II.
(25) Watson, F. H.; Armstrong, A. T.; McGlynn, S. P. *Theor. Chim. Acta* **1970**, *16*, 75–94.
(26) (a) Roothaan, C. C. J. *Rev. Mod. Phys.* **1951**, *23*, 69–89. (b) Hall, G. G. *Proc. R. Soc. London, Ser. A* **1951**, *A205*, 541–552.
(27) Rothenberg, S.; Davidson, E. R. *J. Mol. Spectrosc.* **1967**, *22*, 1–17.

The rotatory strength (velocity form) between electronic states Ψ_K and Ψ_L is defined as the pure imaginary part of the dot product of the electric and magnetic transition moments[28]

$$R^{K,L}(\nabla) = \mathrm{Im}\{(E_L - E_K)^{-1}\langle\Psi_K|\mu(\nabla)|\Psi_L\rangle\cdot\langle\Psi_L|m|\Psi_K\rangle\} \quad (9)$$

where the magnetic dipole operator m is defined as (in atomic units)

$$m = -i\sum_k(\mathbf{r}_k \times \nabla_k) \quad (10)$$

and where the sum is over all electrons. Alternatively, the rotatory strength in the length form is given by

$$R^{K,L}(\mathrm{r}) = \mathrm{Im}\{\langle\Psi_K|\mu(\mathrm{r})|\Psi_L\rangle\cdot\langle\Psi_L|m|\Psi_K\rangle\} \quad (11)$$

So that comparisons can be made between the calculated values, matrix elements using both operator forms will be reported. In the case of calculations using the length form, the origin will be taken at the center of mass.

IV. Spectral and Structural Data

A. Spectral Data. The gas-phase UV absorption spectrum of 3MCB was reported by Rossi and Diversi,[2] where a brief description was given of some band features for the V ← N band. They report the beginning of a strong and broad absorption band at about 6.56 eV, with three shoulders on the low-energy side at 5.96, 6.36, and 6.46 eV. The solution absorption spectrum in *n*-heptane shows two shoulders at 6.36 and 6.46 eV. The similarity between their UV absorption spectra and that of cyclobutene[8] was also noted.

The CD spectrum of 3MCB in *n*-heptane was described as a curve with a negative maximum of strong intensity at 6.49 eV and a shoulder at 6.42 eV. From comparisons with the UV spectrum and the spectra of other monoolefins, they assigned the main CD peak at 6.49 eV to the lowest $S(\pi,\pi^*) \leftarrow S_0$ transition. No assignment was made of the transition giving rise to the shoulder in the CD band.

However, by comparing the UV spectra of cyclohexene,[29] cyclopentene,[29] and cyclobutene,[8] one of the shoulders at the low-energy end of the V ← N band may be reasonably assigned to the $S(\pi,3s) \leftarrow S_0$ transition. It is blue-shifted from cyclohexene to cyclopentene and essentially disappears under the V ← N band in cyclobutene. Further experimental evidence for assignment of this shoulder to the $S(\pi,3s) \leftarrow S_0$ transition was provided by Drake and Mason[30] from CD spectra of olefins in solution.

In more recent theoretical and experimental studies on a similar monoolefin (3MCP), Levi et al.[3] reported both the UV absorption and CD gas-phase spectra for an energy range of about 5.77–8.55 eV. Their absorption spectrum shows a band centered at 6.05 eV, which contains a fine structure interpreted as two vibrational peaks. The CD spectrum shows a negative peak for this band which is also centered at 6.05 eV and also contains two vibrational bands. This band is assigned to the $S(\pi,3s) \leftarrow S_0$ transition. Next, a more intense band appears which peaks at 6.70 eV in the absorption spectrum and has a shoulder at 7.00 eV. Associated with this transition is a positive CD band peaking at 6.70 eV with rotatory strength of +26 (units are centimeter–gram–seconds × 10^{-40}) and is asymmetrically broadened to higher energy. Levi et al. assigned this positive CD band to two transitions, one of which is the $S(\pi,\pi^*) \leftarrow S_0$ transition. Also found was a low-intensity peak in the absorption spectrum at 7.47 eV and a higher intensity peak at 7.80 eV, while the CD spectrum showed a corresponding symmetric, negative peak at 7.70 eV.

From these more recent observations, it appears that assignment of the negative CD peak by Rossi and Diversi at 6.49 eV in 3MCB to the $S(\pi,\pi^*) \leftarrow S_0$ transition needs to be reexamined. One alternative candidate for this assignment is the $S(\pi,3s) \leftarrow S_0$ transition, based on the data cited above.

B. Structure. Since structural data on (*R*)-3-methylcyclobutene are unavailable, an initial geometry was constructed by assembling bond lengths and angles from related molecules,[31,32] which included the assumption that the ring is planar. Since there is sufficient structural dissimilarity between the compounds from which the structural parameters have been taken and (*R*)-3MCB, an energy-refined structure was determined. The geometry optimization, carried out by using the semiempirical SCF method MINDO/3,[33,34] provides evidence supporting an essentially planar ring (i.e., dihedral angle C_2–C_1–C_4–C_3 = 0.54°) for the ground state. However, as pointed out be Dewar et al.,[34] MINDO/3 often predicts a geometry which is too flat for small hydrocarbon rings (e.g., cyclohexane and cyclohexene). Therefore, an additional optimization was carried out by using ab initio SCF calculations with a version of GAUSSIAN 70[35] employing the STO-3G[36] basis set.

Again, an essentially planar geometry (C_2–C_1–C_4–C_3 dihedral angle = 0.65°) for the ring was obtained. The most noticeable difference between the predicted MINDO/3 and GAUSSIAN 70 geometries is the angle formed by the C_3–C_5 (methyl) bond and a line connecting C_1 and C_3, where MINDO/3 predicts an angle formed by C_1–C_3–C_5 (nonbonded angle) to be 138°, while GAUSSIAN 70 predicts 129°. MINDO/3 also predicts slightly longer C–H bond lengths (the largest difference being for C_3–H_4 = 0.034 Å) Since MINDO/3 has reproduced the geometry of cyclobutene[34] quite well and the general agreement between MINDO/3 and GAUSSIAN 70 is reasonably close for 3MCB, especially concerning the ring planarity, the MINDO/3 optimized geometry was employed in all studies. The coordinates for the optimized geometry (from MINDO/3) are given in Table I, and Figure 1 depicts the orientation of the optimized geometry with respect to the coordinate axes.

Table I. Molecular Coordinates (angstroms)[a]

	MINDO/3		
	x	*y*	*z*
C_1	0.0	0.0	0.0
C_2	1.504 18	0.0	0.0
C_3	1.438 14	1.557 44	0.0
C_4	−0.074 18	1.344 33	−0.012 38
C_5	2.146 10	2.409 80	−1.008 72
H_1	−0.716 14	−0.831 11	0.014 81
H_2	2.008 07	−0.462 95	0.882 57
H_3	2.002 18	−0.480 15	−0.873 35
H_4	1.757 78	1.950 46	1.005 77
H_5	3.251 19	2.386 73	−0.892 06
H_6	1.954 90	2.122 33	−2.065 35
H_7	1.861 37	3.481 89	−0.938 64
H_8	−0.886 31	2.083 96	−0.019 60

[a] The optimization method prints the final coordinates to the number of digits reported above.

V. SCF Calculations

The basis sets used in this study are built from linear combinations of normalized primitive spherical Gaussian functions. In general, p-type functions will be of the lobe-function type and, unless otherwise specified, the lobe distance for the *i*th primitive Gaussian, $|R_i|$, is calculated from the relationship $|R_i| = 0.03\alpha_i^{-1/2}$, where α_i is the orbital exponent.[37]

(28) Caldwell, D. J.; Eyring, H. "The Theory of Optical Activity"; Wiley-Interscience: New York, 1971; p 67.
(29) Pickett, L. W.; Muntz, M.; McPherson, E. M. *J. Am. Chem. Soc.* **1951**, *73*, 4862–4865.
(30) Drake, A. F.; Mason, S. F. *Tetrahedron* **1977**, *33*, 937–949.
(31) Herzberg, G. "Electronic Spectra and Molecular Structure: III. Electronic Spectra and Electronic Structure of Polyatomic Molecules"; D. Van Nostrand Reinhold: New York, 1966; pp 629, 646.
(32) Sutton, L. E. "Tables of Interatomic Distances and Configuration in Molecules and Ions"; Burlington House: London, 1958; pp M182, M185.
(33) Baird, N. C.; Dewar, M. J. S. *J. Chem. Phys.* **1969**, *50*, 1262–1274.
(34) Bingham, R. C.; Dewar, M. J. S.; Lo, D. H. *J. Am. Chem. Soc.* **1975**, *97*, 1294–1301.
(35) Hehre, W. S.; Lathan, W. A.; Ditchfield, R.; Newton, M. D.; Pople, J. A. *QCPE* **1984**, No. 26. Modified for Honeywell 66/60 computer by D. Spangler.
(36) Hehre, W. J.; Stewart, R. F.; Pople, J. A. *J. Chem. Phys.* **1969**, *51*, 2657–2664.

Table II. Selected Molecular Orbital Energies and Description

	basis sets[a]											
	MF-FSGO		SZ1		STO-3G		4-31G		DZ		DZD	
description	MO	orbital energy	MO	orbital energy	MO	orbital energy	MO	orbital energy	MO	orbital energy	MO	orbital energy
$\pi^*(2p_z)[C_1-C_4]$											33	0.167
$\pi^*(3p_z)[C_1-C_4]$											26	0.067
$(3p_{x,y})[C_1-C_5]$											25	0.067
$(3p_x)[C_1-C_4]$											24	0.065
3s											20	0.020
$\pi^*[C_1-C]$	20	0.362	20	0.301	20	0.314	20	0.181	20	0.157		
Occupied Molecular Orbitals with Variable Occupancy in CI Calculations												
$\pi[C_1-C_4]$	19	−0.193	19	−0.304	19	−0.290	19	−0.342	19	−0.345	19	−0.346
$\sigma[C_1-C_2,C_3-C_4,C_4-H_8,C_1-H_1]$	18	−0.276	18	−0.392	18	−0.389	18	−0.435	18	−0.439	18	−0.439
$\sigma[C_1-H_1,C_1-C_2,C_2-C_3,$ $C_3-H_4,C_5-H_7]$	17	−0.291	17	−0.408	17	−0.404	17	−0.445	17	−0.447	17	−0.449
$\sigma[C_1-C_2,C_2-H_3,C_3-C_5,$ $C_3-H_4,C_5-H_6]$	16	−0.334	16	−0.446	16	−0.442	16	−0.480	16	−0.483	16	−0.484
$\sigma[C_1-C_2,C_1-C_4,C_2-H_2]$	15	−0.358	15	−0.472	15	−0.464	15	−0.511	15	−0.514	15	−0.515
$\sigma[C_2-H_{2,3},C_5-H_{6,7}]$	14	−0.401	14	−0.511	14	−0.508	14	−0.541	14	−0.543	14	−0.544
$\sigma[C_1-C_2-C_3-C_4-C_1,C_5-H_{5,7}]$	13	−0.420	13	−0.544	13	−0.537	13	−0.573	13	−0.575	13	−0.577
$\sigma[C_2-H_{2,3},C_3-H_4,C_3-C_5,C_5-H_{5,7}]$	12	−0.461	12	−0.583	12	−0.573	12	−0.611	12	−0.613	12	−0.614
$\sigma[C_1-H_1,C_2-H_2,C_3-H_4,C_4-H_8]$	11	−0.543	11	−0.635	11	−0.625	11	−0.669	11	−0.673	11	−0.675
$\sigma[C_1-H_1,C_2-H_3,C_3-H_4,C_4-H_8]$	10	−0.605	10	−0.648	10	−0.655	10	−0.694	10	−0.697	10	−0.698

[a] The descriptions of the occupied MO's with variable occupancy in the CI expansion were qualitatively the same for all six basis sets. Also, the π^* MO was the lowest unoccupied MO, i.e., MO 20, in all five valence basis sets. The virtual MO's which play a major role in the description of the CI wave function and/or in the total value of the calculated rotatory strength will be discussed in the appropriate section. Within the brackets are the bonds which contain most of the MO's electron density.

The five valencelike basis sets are (in increasing number of basis functions) MF-FSGO,[38] SZ1,[39] STO-3G,[36] 4-31G,[40] and DZ.[41] All the above, with the exception of SZ1, have been used to calculate properties on a wide variety of molecules. The SZ1 basis, a recently reported basis set, has its p functions formed from linear combinations of tetrahedrally arranged lobe functions. The MF-FSGO and SZ1 bases have their lobe distances determined by criteria other than the aforementioned relationship to the exponent α_i.[38,39]

A sixth basis set was constructed by adding diffuse s- and p-type functions to the DZ basis set. This provides for the description of Rydberg-like states of 3s and 3p character. To carbons C_1, C_4, and C_5 are added a complete set of noncontracted diffuse p-type functions, analogous to those employed in the studies of Buenker et al.,[15] who performed SCF calculations by using various values of α on several low-lying states in ethylene. For those states in which these diffuse p-type functions made a significant contribution, the value of $\alpha = 0.020$ gave the lowest energy. Also, a pair of noncontracted s-type diffuse functions were placed at the center of the ring. The exponents for these two diffuse functions were chosen to bracket the exponent value corresponding to the minimum energy calculated for the $^1(\pi,3s)$ excited state of ethylene, as reported by Fischbach et al.[17] The two orbital exponents are $\alpha(S1) = 0.020$ and $\alpha(S2) = 0.012$, respectively. Even though the $^1(\pi,3s)$ excited state of ethylene was sensitive to the choice of the orbital exponent for the diffuse function, this same state seemed rather insensitive to the choice of location for the diffuse s-type functions. This basis set is called DZD.

Closed-shell, ab initio SCF calculations were performed on 3MCB by using the six basis sets described above. In Table II are listed the filled MO's, their energies, and a short description of each. Only filled MO's with variable occupancy in the CI procedure are included in the table. In addition, the virtual MO's representing the π^* orbitals are also listed, along with four virtuals from the DZD basis which are important contributors to the CI wave functions.

Table III. Dimensions of Initial $[\Psi^{(1)}]$ and Final $[\Psi^{(2)}]$ CI Wave Functions and the Number of Parent Configurations Used to Generate the Final States

basis set	tot config in $\Psi^{(1)}$	threshold δ_2	tot config in $\Psi^{(2)}$	tot parent config, for $\Psi^{(2)}$
MF-FSGO	27	0.000 090	360	4
SZ1	37	0.000 270	314	4
STO-3G	44	0.000 270	343	4
4-31G	24	0.000 132	479	4
DZ	42	0.000 115	623	6
DZD	22	0.000 040	1112	6

VI. CI Calculations

For a molecule such as 3MCB, performing all possible excitations from the occupied MO manifold into the virtual MO's for all six basis sets was not computationally feasible within the limits of available resources. Instead, a fixed core of nine doubly occupied MO's was used for all basis sets, which included the five MO's describing the five carbon is inner-shells. The additional four core MO's are composed primarily of carbon 2s-type orbitals. There remain ten filled MO's for variable occupancy in the CI calculations, and these were composed primarily of 2p functions (see Table II).

Unlike the filled MO's, the total number of virtual MO's used in the CI calculations is not held constant from one basis set to the next. In the MF-FSGO basis, there are only 6 virtual MO's available, while in the DZD basis there are 60. All virtuals derived from SCF MO calculations using the MF-FSGO, SZ1, and STO-3G basis sets were included in the CI calculations. For the remaining basis sets, the number of virtual orbitals retained in the CI were 21 in the 4-31G, 23 in the DZ, and 20 in the DZD.

CI calculations were performed by using the five valence basis sets to obtain the four lowest singlet states. For the DZD basis set, the lowest five singlet states were calculated. This gave at least one state lying at higher and lower energies than the $^1(\pi,\pi^*)$ state. In order to identify these lowest states, different parent configurations were examined. Once the identities of these 4 or 5 states were known, only the 1 or 2 main contributors to each state were retained as parents, and a new set of initial state

(37) Petke, J. D.; Whitten, J. L.; Douglas, A. W. *J. Chem. Phys.* **1969**, *51*, 256–262.
(38) Christoffersen, R. E. *Adv. Quantum Chem.* **1972**, *6*, 333–393.
(39) Spangler, D.; Christoffersen, R. E. *Int. J. Quantum Chem.* **1980**, *17*, 1075–1097.
(40) Ditchfield, R.; Hehre, W. J.; Pople, J. A. *J. Chem. Phys.* **1971**, *54*, 724–728.
(41) Snyder, L. C.; Basch, H. "Molecular Wave Functions and Properties"; Wiley-Interscience: New York, 1972; pp 20–32.

Table IV. CI Calculations: Composition of Singlet States, Description of Parent Configurations, and Ground-State Energies

basis set	state	label[a]	composition[b]	parent config	ground-state energies, au
MF-FSGO	S_0	(G.S.)	0.98(SCF), −0.15(19²–20²)	(SCF), (17–20), (18–20), (19–20)	−165.478 36
	S_1	(σ_{18},π^*)	−0.75(18–20), 0.53(17–20), 0.26(19–20), 0.14(18,19–20²), −0.13(13–20), 0.12(16–20)		
	S_2	(π,π^*)	−0.90(19–20), 0.36(18–20)		
	S_3	(σ_{17},π^*)	−0.69(17–20), −0.39(18–20), 0.38(15–20), −0.31(16–20)		
SZ1	S_0	(G.S.)	−0.97(SCF), 0.20(19²–20²)	(SCF), (15–20), (18–20), (19–20)	−187.416 26
	S_1	(σ_{18},π^*)	−0.92(18–20), 0.13(15–20), −0.11(10–20), 0.10(11,19–20²)		
	S_2	(π,π^*)	−0.95(19–20), 0.10(17–20)		
	S_3	(σ_{15},π^*)	−0.76(15–20), 0.46(17–20), 0.27(13–20), −0.21(14–20), 0.15(11–20), 0.13(12–20), −0.11(19–20)		
STO-3G	S_0	(G.S.)	0.96(SCF), −0.22(19²–20²)	(SCF), (15–20), (18–20), (19–20)	−191.686 15
	S_1	(σ_{18},π^*)	0.92(18–20), −0.17(16–20), −0.11(10–20), 0.11(11,19–20²), 0.10(15–20)		
	S_2	(π,π^*)	−0.94(19–20), 0.11(18–22), 0.11(15–32)		
	S_3	(σ_{15},π^*)	−0.85(15–20), 0.32(13–20), 0.26(16–20), −0.19(17–20), −0.12(14–20), 0.10(18,19–20²)		
4-31G	S_0	(G.S.)	−0.98(SCF), 0.16(19²–20²)	(SCF), (16–20), (18–20), (19–20)	−193.680 59
	S_1	(σ_{18},π^*)	−0.85(18–20), 0.36(19–20), −0.20(16–20)		
	S_2	(π,π^*)	0.89(19–20), 0.35(18–20)		
	S_3	(σ_{17},π^*)	0.83(17–20), −0.32(15–20), 0.25(14–20), 0.19(11–20), −0.13(12–20)		
DZ	S_0	(G.S.)	0.97(SCF), −0.17(19²–20²)	(SCF), (16–20), (18–20), (19–20), (19–21), (19–22)	−193.886 16
	S_1	(σ_{18},π^*)	−0.85(18–20), −0.33(19–20), 0.23(16–20), 0.12(15–20)		
	S_2	(π,π^*)	−0.91(19–20), 0.31(18–20)		
	S_3	(π,σ_{21}^*)	0.91(19–21), −0.28(19–22), 0.12(19–25)		
DZD	S_0	(G.S.)	−0.98(SCF), 0.13(19²–20²)	(SCF), (19–20), (19–24), (19–25), (19–26), (19–33)	−193.884 14
	S_1	(π,3s)	−0.93(19–20), −0.24(19–32)		
	S_2	($\pi,3p_x$)	−0.75(19–24), 0.42(19–26), 0.34(19–21), −0.29(19–25), −0.11(19–33), 0.11(19–20)		
	S_3	(π,π^*)	−0.79(19–26),[d] −0.45(19–24), 0.20(19–21), 0.20(19–25), −0.16(19–29), 0.15(19–33),[e] −0.11(19–32)		
	S_4	($\pi,3p_{x,y}$)[c]	−0.91(19–25), 0.31(19–26), 0.17(19–24), 0.11(19–30)		

[a] For example, $S_1[\sigma_{18},\pi^*]$ represents the character of the dominant configuration, i.e., (18–20), listed in that state's composition. [b] Included states with CI coefficients $\geq|0.1|$. The parentheses contain the labels of the orbital from Table II which is involved in the substitutions to form the configurations. (SCF) is the configuration consisting of the SCF determinant. A singly substituted configuration is represented by (a–b), where spin–orbital "b" is substituted for spin–orbital "a". The doubly substituted configurations are represented by (a^2–b^2) where both the α and β spin parts of "a" are replaced by the α,β spin parts of "b" (a,b–c^2) represents the case where spin–orbital "a" and "b" are replaced by both the α and β spin parts of spin–orbital c, not necessarily in that order. [c] Represents a state comprised of a large contribution from functions on carbons C_1 and C_5. [d] MO 26 is a π^*-antibonding orbital consisting primarily of the diffuse $3p_z$ functions on C_1 and C_4. [e] MO 33 is also a π^*-antibonding orbital but consists parimarily of the valencelike $2p_z$ functions on C_1 and C_4.

descriptions were calculated, each containing less than 50 configurations. From these new parents and initial-state descriptions, the final-state wave functions were calculated.

Table III lists the number of configurations used for each basis set in the initial and final wave functions $\Psi^{(1)}$ and $\Psi^{(2)}$, respectively, and also the number of parent configurations and energy thresholds (δ_2) used to generate the final set of configurations in $\Psi^{(2)}$. Table IV contains configurational compositions of the low-lying singlet states: S_0–S_3 for the valence basis sets and S_0–S_4 for the DZD basis set. Only those configurations with CI coefficients $\geq$0.1 are included. A singly substituted configuration is represented by (a–b), where spin–orbital "b" is substituted for spin–orbital "a". Doubly substituted configurations are represented by (a^2–b^2).

A. Valence Basis Sets: State Compositions. From Table IV it can be seen that the two lowest excited states are the same in all five valence-like basis sets. The lowest excited state is described primarily as an (18–20) excitation which, as noted in the table, is a (σ_{18},π^*) configuration. Thus, not only is there a low-lying $^1(\sigma,\pi^*)$ state, but it is predicted to be the lowest lying singlet when valence-like basis sets are used. This is similar to the results of Robin et al.,[42] where calculations using a valence basis set and no CI predicted the lowest excited singlet state in ethylene to be an excitation of an electron from the C–H σ-bonding MO into the π^* MO, i.e., $S_1(\sigma_{CH},\pi^*)$. The σ_{CH} MO is analogous to MO 18 used here. But, upon the addition of diffuse functions, the $^1(\sigma_{CH},\pi^*) \leftarrow S_0$ transition in ethylene remained essentially unchanged while the $^1(\pi,\pi^*) \leftarrow S_0$ transition fell to an energy below that of the $^1(\sigma_{CH},\pi^*) \leftarrow S0$ transition.

Because of the results of Robin et al., a question arises as to whether the $S_1(\sigma_{18},\pi^*)$ state is the lowest lying singlet excited state in 3MCB. If the inclusion of diffuse functions in the DZD calculation considerably separates these two states in energy, then the amount of intensity the $^1(\pi,\pi^*) \leftarrow S_0$ transition borrows from the $^1(\sigma_{18},\pi^*) \leftarrow S_0$ transition could be significantly altered.

To illustrate the changes in electron density that are implied by the use of MO's 18–20, Figure 2 depicts MO electron density contour plots of MO's 18–20. MO 18 is a σ MO, while MO's 19 and 20 are π MO's. As indicated in Table IV, these MO's are predominant contributors to the low-lying states.

The configurational character of S_3 changes for the different basis sets. For the MF-FSGO and 4-31G basis sets, this state is described predominantly by a (17–20) configuration and is of (σ_{17},π^*) character. Alternatively, S_3 in the SZ1 and STO-3G basis sets is described primarily by a (15–20) configuration, yielding a $S_3(\sigma_{15},\pi^*)$ state, while the DZ basis gives an S_3 state, having an $S_3(\pi,\sigma^*_{21})$ character. The character of the σ bonds described by MO's 15 and 17 are given in Table II. Such disparate descriptions of this higher lying state illustrate the inability of the limited basis sets/CI studies to describe this transition reliably.

B. Valence Basis Sets: Transition Properties. Let us begin by examining the $S_2(\pi,\pi^*) \leftarrow S_0$ transition, which is of particular interest in the current study. In Table V the energy for this transition in all the basis sets is seen to be considerably above the

(42) Robin, M. B.; Hart, R. R.; Kuebler, N. A. *J. Chem. Phys.* **1966**, *44*, 1803–1811.

Table V. CI Calculations: Singlet–Singlet Transition Energies, Oscillator Strengths, and Rotatory Strengths

		CI results					
			transition	oscillator strengths[a]		rotatory strengths[b]	
basis set	state	label	energies, eV	$f(r)$	$f(\nabla)$	$R(r)$	$R(\nabla)$
MF-FSGO	S_1	$[\sigma_{18},\pi^*]$	9.714 58	0.031	0.029	−73.0	−63.4
	S_2	$[\pi,\pi^*]$	9.900 41[c]	0.347[d]	0.211	+30.0[e]	+31.3
	S_3	$[\sigma_{17},\pi^*]$	10.368 69	0.050	0.034	+62.6	+55.4
SZ1	S_1	$[\sigma_{18},\pi^*]$	10.779 13	0.006	0.004	−7.43	−2.54
	S_2	$[\pi,\pi^*]$	11.536 56	0.325	0.102	+8.75	+10.6
	S_3	$[\sigma_{15},\pi^*]$	12.147 20	0.011	0.004	+5.81	−1.84
STO-3G	S_1	$[\sigma_{18},\pi^*]$	10.843 81	0.007	0.004	−7.81	−1.80
	S_2	$[\pi,\pi^*]$	11.470 19	0.290	0.086	+.067	+4.09
	S_3	$[\sigma_{15},\pi^*]$	12.106 00	0.001	0.001	+.459	−2.58
4-31G	S_1	$[\sigma_{18},\pi^*]$	9.059 08	0.042	0.018	−115.0	−73.9
	S_2	$[\pi,\pi^*]$	9.165 88	0.260	0.131	+83.9	+62.3
	S_3	$[\sigma_{17},\pi^*]$	10.816 31	0.015	0.009	+25.2	+15.3
DZ	S_1	$[\sigma_{18},\pi^*]$	8.731 73	0.033	0.014	−107.0	−62.1
	S_2	$[\pi,\pi^*]$	8.911 22	0.291	0.135	+95.6	+61.3
	S_3	$[\pi,\sigma_{21}^*]$	10.093 70	0.010	0.011	−6.17	−5.48
DZD	S_1	$[\pi,3s_{20}]$	7.144 05	0.015	0.009	−5.11	−2.19
	S_2	$[\pi,3p_{x_{24}}]$	7.977 35	0.024	0.015	+11.7	+9.25
	S_3	$[\pi,\pi_{26}^*]$	8.184 25	0.050	0.025	+2.86	+4.00
	S_4	$[\pi,3p_{x,y}]$	8.249 36	0.010	0.006	−6.54	−5.03

[a] $f(r)$ is calculated by using the length form of the electric dipole operator while $f(\nabla)$ uses the velocity form. See eq 7 and 8. The origin for all dipole moments is taken as the center of mass unless otherwise specified. [b] Rotatory strengths are calculated by using the length $[R(r)]$ and velocity $[R(\nabla)]$ forms of the electric dipole operators. See eq 9 and 11. The rotatory strengths are in units of centimeter–gram–second × 10^{-40}. [c] The experimental transition energy for the $^1[\pi,\pi^*]$ transition in (*R*)-3MCB is reported to be approximately 6.5 eV. [d] The experimental oscillator strength in cyclobutene for the $^1[\pi,\pi^*]$ transition is approximately 0.28 (see ref 8) and for (*R*)-3MCP is ~0.16 (see ref 3). [e] The experimental rotatory strength for the similar monoolefin (*R*)–3MCP is +26 (units of centimeter–gram–second × 10^{-40}), but this probably includes another transition in addition to the $^1[\pi \rightarrow \pi^*]$ transition.

experimental value reported by Rossi and Diversi (6.5 eV), ranging from 8.9 (DZ basis) to 11.5 eV (SZ1 basis).

The experimental oscillator strength for the ($\pi \rightarrow \pi^*$) transition in cyclobutene is $f = 0.28$[8] and for 3MCP is $f = 0.16$.[3] Thus, while not known experimentally, a calculated oscillator strength for 3MCB in the range of 0.16 to 0.28 would be reasonable. Data in Table V show that the length form of the electric dipole operator typically gives oscillator strengths which lie at the high end of this range. The values vary from $f(r) = 0.26$ for the 4-31G basis to 0.35 for the MF-FSGO basis. These values each compare favorably with the value obtained for the largest nondiffuse basis set, DZ, where $f(r) = 0.29$. The velocity form of the dipole moment operator gives consistently lower oscillator strengths than the length form. They range from $f(\nabla) = 0.09$ for the STO-3G basis to 0.21 for the MF-FSGO basis. This difference in f values for the two forms of the operator is due, in part, to the high values calculated for the transition energies. From eq 7 and 8, we see that high transition energies will lower the $f(\nabla)$ value, while they will raise the value of $f(r)$. To illustrate this effect, the oscillator strengths were recalculated by using a transition energy of E = 6.5 eV, which is approximately the onset of the V ← N band in cyclobutene. The five basis sets give values for $f(r)$ and $f(\nabla)$ of 0.23 and 0.43 in MF-FSGO, 0.18 and 0.18 in SZ1, 0.17 and 0.15 in STO-3G, 0.19 and 0.18 in 4-31G, and 0.21 and 0.18 in the DZ. The two forms are now in better agreement with one another and with oscillator strengths observed experimentally in cyclobutene and 3MCP.

There remains a question as to how much of the V ← N band intensity is due to the transition to the $S_2(\pi,\pi^*)$ state, especially since the $S(\pi,3s) \leftarrow S_0$ transition also seems to lie under the broad V ← N band in cyclobutene. In addition, the $S(\pi,3p_y) \leftarrow S_0$ transition is also predicted to lie under the V ← N band and becomes electric dipole allowed in 3MCB and 3MCP due to the lack of strict spatial symmetry and, in cyclobutene, with twisting about the double bond. This could also contribute to the experimental oscillator strength normally assigned only to the $S(\pi,\pi^*) \leftarrow S_0$ transition.[13,15,17-19] Thus, the experimental values themselves are subject to these additional uncertainties.

Values for both forms of the rotatory strength $R(r)$ and $R(\nabla)$, are also given in Table V. Unless otherwise stated, all properties are calculated with respect to the center of mass of the molecule. For the transition to the $S_2(\pi,\pi^*)$ state, all five rotatory strengths

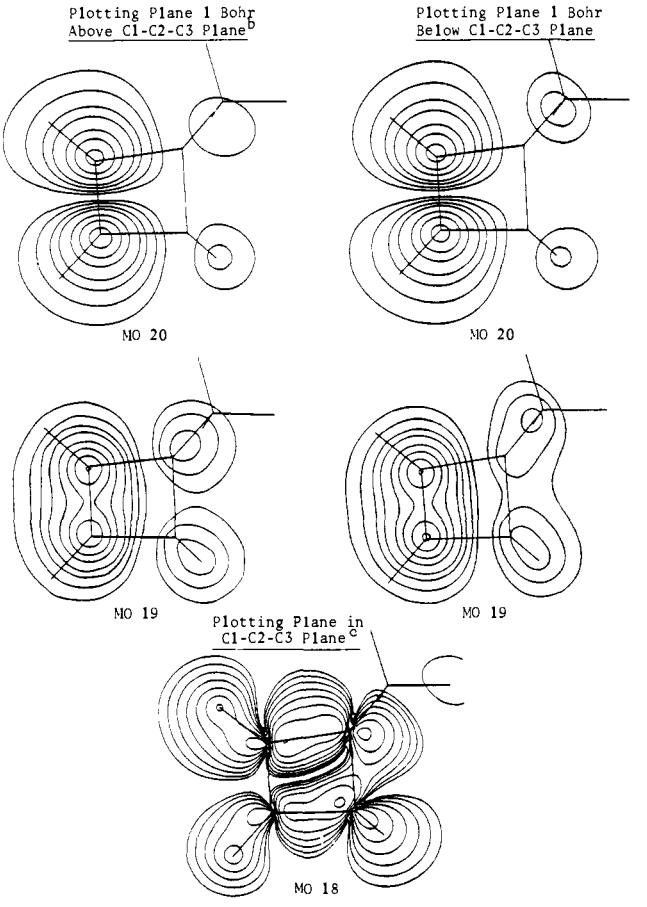

Figure 2. Electron density plots of MO's 18(σ), 19(π), and 20(π). Taken from the results of the DZ basis set. Superscript a denotes that the methyl group is below the approximate plane of the ring for all the above plots. Superscript b denotes that the contour lines for MO's 19 and 20 have the values 0.001, 0.003, 0.007, 0.012, 0.025, 0.040, 0.060, 0.080, 0.100, 0.200, and 0.400 in units of electrons per bohr.[3] Superscript c denotes that the contour lines for MO 18 have the values 0.001, 0.002, 0.004, 0.008, 0.016, 0.032, 0.064, 0.128, 0.256, 0.512, and 1.024 in units of electrons per bohr.[3]

Table VI. Transition Dipole Moment Contributions of Configurations (18–20) and (19–20) for the Transition to the $^1[\pi,\pi^*]$ State

		Matrix Element Transition Dipole Contribution[b]										
	matrix[a]	magnetic			electric-length form			electric-velocity form				
basis set	element description	x	y	z	x	y	z	x	y	z	R(r)	$R(\nabla)$
MF-FSGO	(19–20)	+0.1527	+0.0089	+0.8644	+0.0708	−1.7270	−0.0085	+0.0127	−0.3765	−0.0009	−0.0118	−0.0021
	(18–20)	−0.0278	−0.1340	+0.0117	−0.0074	+0.0175	+0.0445	−0.0024	+0.0050	+0.0262	−0.0016	−0.0003
	(19–20) + (18–20)	+0.1250	−0.1251	+0.8761	+0.0633	−1.7096	+0.0360	+0.0103	−0.3715	+0.0253	+0.2532	+0.0697
	full CI wave function	+0.1677	−0.0868	+1.1046	+0.0097	−1.1953	+0.0199	−0.0028	−0.3389	+0.0175	+0.1272	+0.0483
SZ1	(19–20)	−0.0998	−0.0300	−0.7032	−0.1145	+1.7367	+0.0225	−0.0193	+0.2997	+0.0044	−0.0565	−0.0100
	(18–20)	+0.0012	+0.0491	−0.0049	−0.0059	+0.0025	−0.0189	−0.0011	+0.0005	−0.0060	+0.0001	−0–
	(19–20) + (18–20)	−0.0986	+0.0191	−0.7081	−0.1204	+1.7892	+0.0036	−0.0204	+0.3002	−0.0016	+0.0198	+0.0088
	full CI wave function	+0.0742	+0.0310	−1.0783	−0.0420	+1.0721	−0.0065	−0.0146	+0.2544	−0.0113	+0.0371	+0.0189
STO-3G	(19–20)	+0.0980	+0.0247	+0.6550	+0.1053	−1.7126	−0.0205	+0.0171	−0.2843	−0.0043	−0.0454	−0.0082
	(18–20)	−0.0012	−0.0413	+0.0034	+0.0029	−0.0013	+0.0166	+0.0004	−0.0003	+0.0050	−0–	−0–
	(18–20) + (19–20)	+0.0969	−0.0166	+0.6583	+0.1081	−1.7139	−0.0038	+0.0175	−0.2846	+0.0007	+0.0363	+0.0067
	full CI wave function	+0.0065	−0.0038	+1.0432	−0.0021	−1.0150	−0.0034	−0.0087	−0.2327	+0.0062	+0.0003	+0.0072
4-31G	(19–20)	+0.1339	+0.0819	+0.7999	+0.0650	−1.7106	−0.0083	+0.0091	−0.3227	−0.0023	−0.1379	−0.0270
	(18–20)	−0.0117	−0.2315	+0.0479	+0.0090	−0.0009	+0.1036	+0.0009	+0.0006	+0.0282	+0.0005	+0.0012
	(18–20) + (19–20)	+0.1222	−0.1496	+0.8478	+0.0740	−1.7144	+0.0953	+0.0100	−0.3221	+0.0259	+0.3461	+0.0712
	full CI wave function	+0.0941	−0.3138	+1.0816	−0.0371	−1.0759	+0.0202	−0.0248	−0.2560	+0.0101	+0.3560	+0.0889
DZ	(19–20)	+0.1175	+0.0211	+0.8274	+0.0786	−1.7933	−0.0026	+0.0094	−0.3279	−0.0008	−0.0307	−0.0064
	(18–20)	−0.0088	−0.2306	+0.0342	+0.0269	−0.0025	+0.0598	+0.0076	−0.0005	+0.0111	+0.0023	+0.0004
	(18–20) + (19–20)	+0.1087	−0.2095	+0.8616	+0.1055	−1.7958	+0.0572	+0.0170	−0.3285	+0.0102	+0.4368	+0.0793
	full CI wave function	+0.0484	−0.3482	+1.1812	+0.0203	−1.1540	+0.0025	−0.0006	−0.2578	−0.0039	+0.4056	+0.0851

[a] The matrix element contribution to the dipole moments is between the Φ_{SCF} configuration and the configuration listed in this column. For example, (19–20) represents the matrix element between configurations Φ_{SCF} and Φ_{19-20} which are the main contributors to the (G.S.) and $^1[\pi,\pi^*]$ states, respectively. All matrix element values include the CI coefficients. The last two columns give the calculated scalar product of the dipole transition matrix element of the SCF configuration with the configuration listed in column two. [b] All matrix elements are in atomic units.

are seen to be positive, indicating a lack of sensitivity of the calculated sign to the choice of the valence-like basis set. However, the positive CD predicted by the current calculations is of opposite sign to that reported by Rossi and Diversi[2] for the band which they assign to the $S(\pi,\pi^*) \leftarrow S_0$ transition. But, this calculated sign is consistent with the positive CD band reported for the $S(\pi,\pi^*) \leftarrow S_0$ transition in 3MCP.[3]

The ground-state wave functions obtained from the CI calculations (see Table IV) have an expected large contribution from the SCF determinant, while the $S_2(\pi,\pi^*)$ state is labeled as such because configuration (19–20), which represents a promotion of an electron from a filled π MO to a virtual π^* MO, has the largest CI coefficient in that state. It is then implied that the electronic distribution is primarily described in the ground state by the SCF determinant and in the $S_2(\pi,\pi^*)$ state by the determinant (19–20). A check on the relative importance of the main contributors to the full CI expansion is how well properties can be calculated by using only the main contributor to each state. This can then be compared to the same property calculated by using the total CI wave function.

This check is reported in Table VI, which includes a listing of calculated magnetic and electric transition dipole moments. The moments are calculated between configurations (including their coefficients) of the ground-state and $S_2(\pi,\pi^*)$ excited-state CI wave functions. Interestingly, it is found that the dot product of the electric and magnetic transition dipole moments for the matrix elements between the $\Phi_{(SCF)}$ and $\Phi_{(19-20)}$ configurations has a negative sign for both R(r) and $R(\nabla)$ in all the valence basis sets.

However, when contributions from other configurations [e.g., (18–20)] are included, the sign is seen to be positive and in agreement with the sign calculated for the overall wave function. This result illustrates two points of interest. First, even though one configuration may dominate the overall state description, use of that configuration alone may not be sufficient to ensure even the correct sign of the calculated CD transition, relative to the sign predicted by the overall CI wave function. Second, for the particular case of 3MCB we note that since $\Phi_{(18-20)}$ is the main contributing configuration to the lowest energy excited state, the transition $S_2(\pi,\pi^*) \leftarrow S_0$ borrows intensity from the $S_1(\sigma_{18},\pi^*) \leftarrow S_0$ transition and is significant in determining the sign of the calculated rotatory strength.

Another point which should be noted is the inherent sensitivity of the calculated rotatory strength in a nearly symmetric molecule to the selection of configurations in the CI wave function. The ring in 3MCB is nearly planar and hence lies essentially in the x–y plane of the coordinate axes. If the molecule is thought of initially as planar cyclobutene, and if the molecule is shifted so that the origin lies in the center of the π bond, one finds that only the electric y component and magnetic z components of the $S(\pi,\pi^*) \leftarrow S_0$ transition dipole moments can be nonzero by symmetry arguments, with this orthogonality in the dipole moments making the molecule optically inactive. However, the methyl group perturbs the otherwise C_{2v} spatial symmetry, and if the perturbation is small, one would still expect the electric y component and magnetic z component to be large compared to the remaining two components in each transition dipole moment. Examination of Table VI shows that, for the transition to the $^1(\pi,\pi^*)$ state, the electric y component and magnetic z component between configurations $\Phi_{(SCF)}$ and $\Phi_{(19-20)}$ are indeed much larger than the remaining two components for all the valence basis sets.

Problems then arise because of the definition of the rotatory strength as involving the dot product of the electric and magnetic moments. As shown earlier, it is the small y component of the magnetic moment that is multiplied by the large y component of the electric moment. Likewise, it is the small z component of the electric moment that is multiplied by the large z component of the magnetic moment. The overall electric z component from important matrix elements is frequently so small in magnitude that contributions from other configurations which have a significantly smaller contribution to the CI wave function (as determined from the square of their CI coefficients) can easily reverse the sign of the electric z component as these other matrix elements are added to form the total electric transition dipole moment. This is indeed what happened in the current CI studies. The small electric z component and small magnetic y component have signs determined by the contribution to the dipole moments from the configuration $\Phi_{(18-20)}$ which were only a secondary contributor to the $^1(\pi,\pi^*)$ state wave function [as displayed by the small value (less than 0.01) of the CI coefficients]. This indicates that the calculated rotatory strengths in a nearly symmetric molecule can be very sensitive to the CI wave functions, even to the extent that configurations which contribute to the CI wave function with

Table VII. Comparison of Observed Spectrum in the Monoolefin (*R*)-3MCP with the Calculated Spectrum in (*R*)-3MCB from the DZD CI

exptl (*R*)-3MCP[a]			theoretical (*R*)-3MCB					
ΔE, eV	R^b	f	ΔE, eV	transition	$R(r)^b$	$R(\nabla)$	$f(r)$	$f(\nabla)^c$
6.05	−16	0.03	7.14	$S_1[\pi,3s_{20}] \leftarrow S_0$	−5.1	−2.2	0.015	0.009
6.7			7.98	$S_2[\pi,3px_{24}] \leftarrow S_0$	+12	+9.3	0.024	0.015
	+26	0.16	8.18	$S_3[\pi,\pi_{26}] \leftarrow S_0$	+2.9	+4.0	0.050	0.025
7.0			8.25	$S_4[\pi,3p_{x,y}] \leftarrow S_0$	−6.5	−5.0	0.010	0.006

[a] see ref 3. [b] In units of 10^{-40} centimeter-gram-second. See eq 11. [c] see eq 7.

coefficients less than 0.01 can still be important in determining the rotatory strengths for some transitions. This also implies a need to include more states in the CI wave function than simply the two involved in the transition, so as to allow for small but important state mixings.

C. DZD Basis Set: State Compositions. The DZD basis was also used in an SCF and CI calculation, and the CI study was carried out in the same fashion as described for the valence-like basis sets. The size of the CI wave function and the parents used are listed in Table III. In Table IV are listed the compositions of the five lowest singlet states. The first excited singlet is an $S_1(\pi,3s)$ state involving an excitation into MO 20, which is the more diffuse of the two 3s-type basis functions. The next singlet is an $S_2(\pi,3p_x)$ state, which is primarily an excitation into the diffuse $3p_x$ basis functions on C_1 and C_4. The $S_3(\pi,\pi^*)$ state is the next highest singlet state and is primarily described by configuration (19–26), MO 26 being the antibonding combination of diffuse $3p_z$ basis functions on C_1 and C_4. Of the remaining six configurations listed for the $^1(\pi,\pi^*)$ state, only (19–33) is valence-like, MO 33 being primarily an antibonding combination of $2p\pi$ basis functions on C_1 and C_4. The $S_3(\pi,\pi^*)$ state thus appears to be quite diffuse [even though labeled a (π,π^*) state] as seen by the relatively large CI coefficient of −0.79 for $\Phi_{(19-26)}$, while the valence-like configuration, $\Phi_{(19-33)}$, has a coefficient of only 0.15. The highest calculated excited state is an $S_4(\pi,3p_{x,y})$ state, which is primarily described by MO 25. This MO consists of $3p_x$ and $3p_y$ basis functions on carbon C_1 and the methyl carbon C_5. It should be noted that none of the four lowest excited states is predicted to be valence-like in character nor is any of the $^1(\sigma,\pi^*)$ type in contrast to the results described in the previous section for basis sets restricted to valence-like basis functions.

In Figure 3, comparison is made between excited states calculated for the DZD basis and those calculated for ethylene by Buenker and Peyerimhoff,[13] who used a basis including double-ζ plus diffuse functions and s- and p-type polarization functions on the C–C bond. The ordering of the three lowest singlet excited states in 3MCB match quite well with the three lowest singlet states in ethylene. The $S_4(\pi,3p_{x,y})$ state is not expected to correlate with any ethylene excited state, since the $^1(\pi,3p_{x,y})$ state has a large contribution from the carbon atom of the methyl group, which is not present in ethylene.

The calculated results indicate that the low-lying $S_1(\sigma_{18},\pi^*)$ state which is present in the other basis sets is not one of the five lowest states. Other CI calculations using the DZD basis including parent configurations $\Phi_{(18-26)}$ and $\Phi_{(18-33)}$ do not generate a significant number of new configurations, and the results obtained from these calculations are unchanged from the original calculation. Therefore, an unambiguous determination of the importance of the $S(\sigma_{18},\pi^*)$ state to the spectral features of 3MCB must await further study.

An interesting result from the DZD calculation is the fact that the $S_3(\pi,\pi^*)$ state has far more Rydberg (diffuse) character than predicted by the aforementioned experimental and theoretical evidence for ethylene. This can be seen by comparing the square of the CI coefficient (0.62) for the diffuse configuration $\Phi_{(19-26)}$ with that (0.02) of the valence-like configuration $\Phi_{(19-33)}$. By comparison to ethylene,[13] however, it is expected that further expansion of the basis and alteration of the MO's used in the CI study would lead to increased valence character.

A similar result was found by Buenker and Peyerimhoff[13] in ethylene by using a basis set of DZD-plus polarization functions. Their single and double excitation CI produced an oscillator

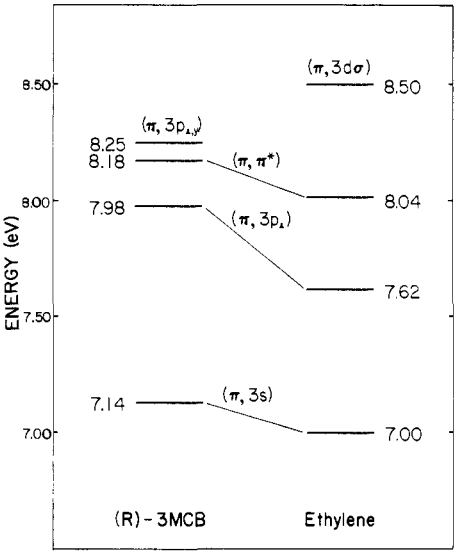

Figure 3. Comparison of the calculated singlet-state ordering from DZD-CI with the state ordering for ethylene as calculated by Buenker and Peyerimhoff. See ref 13 and 23. The coordinate system used by Buenker and Peyerimhoff has been changed to be consistent with the orientation of the ethylenic bond in (*R*)-3-methylcyclobutene in the coordinate system used here.

strength of $f(r) = 0.06$ for the $^1(\pi \rightarrow \pi^*)$ transition when the canonical π^* SCF-MO was used [obtained from an SCF calculation on the $^1(\pi,\pi^*)$ state] as a basis for the CI orbitals. But by employing the natural orbitals obtained from an initial CI wave function on the lowest $^1(\pi,\pi^*)$ state, the value for $f(r)$ rose to 0.260, indicating a much less diffuse $^1(\pi,\pi^*)$ state. The canonical π^* SCF-MO seems ill-suited for use as a basis orbital in the CI calculation on the $^1(\pi,\pi^*)$ state in ethylene, producing a state which is too diffuse. This appears also to happen here in 3MCB, where the canonical π^* SCF-MO is used in the CI. This would, of course, be avoided in the case of a full CI, suggesting the further exploration with better (i.e., more complete) CI expansions and testing the effects of natural orbitals on such monoolefins.

D. DZD Basis Set: Transition Properties. The energy of 8.2 eV for the $S_3(\pi,\pi^*) \leftarrow S_0$ transition in Table V shows a lowering of about 0.73 eV for the DZD basis compared to that calculated by the DZ basis. This still lies far above the reported experimental value of approximately 6.5 eV. Also the calculated oscillator strengths in Table V, $f(r) = 0.050$ and $f(\nabla) = 0.025$, are far below the experimental oscillator strength of $f = 0.28$ and $f = 0.16$ reported for cyclobutene and 3MCP, respectively. These oscillator strengths differ more from the experimental estimate than the oscillator strengths calculated from any of the valence basis sets. Judging from the low oscillator strength in the DZD calculation and the analysis of the wave function in the previous section, the $S(\pi,\pi^*)$ state in this basis apparently assumes more Rydberg character than is actually present in the molecule.

It is of interest to compare the signs of the rotatory strengths and energies of the transitions calculated by using the DZD basis with the experimental absorption and CD spectra of the similar monoolefin 3MCP, since reexamination of assignments of transitions made earlier has been indicated. In Table VII we see the energy ordering and rotatory strengths determined with the DZD basis for the four lowest calculated transitions, along with the

experimental CD bands reported for 3MCP.

The rotatory strength for the calculated $S_1(\pi,3s) \leftarrow S_0$ transition in 3MCB is seen to be negative, which agrees in sign with the lowest energy CD peak centered around 6.05 eV in 3MCP. The next experimental absorption band and its corresponding CD band (in increasing transition energy) has its maximum at 6.70 eV, and the CD peak is positive in sign and reported to be asymmetrically broadened to higher energy. Levi et al.[3] assign this peak at 6.70 eV to two transitions, the $S(\pi,\pi^*) \leftarrow S_0$ valence transition and an $S(\pi,3p_z) \leftarrow S_0$ Rydberg transition (transformed to the current coordinate system, where the $3p_z$ basis functions are in the same direction as the $2p\pi$ basis functions). This could account for the asymmetric broadening of this peak. They acknowledge that the methods they used could have forced an artificial splitting of the $^1(\pi,\pi^*)$ state into two separate states, with one being valence and the other Rydberg in nature. This could happen due to the use of the lowest $^3(\pi,\pi^*)$ state as the spatial representation for the lowest $^1(\pi,\pi^*)$ state. And, as they mention, the true lowest $^1(\pi,\pi^*)$ state is more spatially diffuse than the lowest $^3(\pi,\pi^*)$ state.[12,15,23,43] However, they conclude that both states exist, based upon the rationale that their next higher energy $^3(\pi,\pi^*)$ state is "Rydberg-3p" in character.

The current results indicate that this experimental band system would best be associated with the remaining three calculated transitions in 3MCB. These transitions lie very close to one another, with their order being (in increasing ΔE) $S(\pi,3p_x) \leftarrow S_0$, $S(\pi,\pi^*) \leftarrow S_0$, and $S(\pi,3p_{x,y}) \leftarrow S_0$. The associated transition energies are 7.98, 8.18, and 8.25 eV, respectively. The corresponding rotatory strengths for these calculated transitions are [given in pairs of $R(r)$, $R(\nabla)$] +11.7, +9.25, +2.85, +4.00, and −6.54, −5.03, respectively. The question of whether these states will remain so closely bunched together if the basis set is improved can be partially answered by using the results from an ethylene calculation by Buenker and Peyerimhoff.[13] In that study CI calculations were performed on the ground and $^1(\pi,\pi^*)$ states by using first a DZD basis and then DZD-plus polarization functions, which were placed on the carbon–carbon bond. Their results showed a decrease in the calculated ΔE's for the Rydberg state of approximately 0.10 eV, while the transition energy to the $^1(\pi,\pi^*)$ state decreased by 0.18 eV. Similar shifts in the calculated $^1(\pi,3p_y)$, $^1(\pi,\pi^*)$, and $^1(\pi,3p_{x,y})$ states in 3MCB would still leave them lying close to one another and the energy orderings unchanged.

The sums of the calculated rotatory strengths over the three transitions for the two operator forms are $R(r) = +8.0$ and $R(\nabla) = +8.2$. The positive signs for these rotatory strength summations are consistent with the positive sign of the experimentally observed CD peak at 6.70 eV in 3MCP. Having these three transitions so close to one another would also explain the asymmetric broadening seen in the experimental peak. Thus, the current calculated results for 3MCB are seen to be consistent with the experimental results for 3MCP but are in disagreement with the experimental assignment of transitions in 3MCB given by Rossi and Diversi.[2]

VII. Conclusions

A. Basis Set Dependence. Within the valence basis sets, the calculated sign of the R values is indeed stable. The CI calculations give positive $R(r)$ and $R(\nabla)$ values in all the basis sets for the transition to the $^1(\pi,\pi^*)$ state, although the magnitudes vary considerably, ranging from $R(r) = +0.067$ for STO-3G to +95.6 for DZ (see Table V). The DZD basis (which includes diffuse functions) calculates the same state ordering for the lowest four states as that found in ethylene.

B. Assignment of Transitions. The DZD basis predicts a positive rotatory strength for the transition to the $^1(\pi,\pi^*)$ state, which is consistent with the valence basis sets but is in contradiction to the experimental assignment of Rossi and Diversi. In addition, the DZD calculations give a negative sign for the transition to the $^1(\pi,3s)$ Rydberg state. These results essentially agree with those from the recent theoretical and experimental study by Levi et al.[3] on 3MCP, which also assigns a negative CD band to the transition to the $^1(3s,\pi)$ state and a positive CD band, at least in part, to the $S(\pi,\pi^*) \leftarrow S_0$ transition. Other states in the same vicinity as the $^1(\pi,\pi^*)$ state include the $^1(\pi,3p_x)$ and $^1(\pi,3p_{x,y})$ states.

C. R(r) vs. R(∇). In comparing the two different electric dipole operator forms for use in R, it is shown in Table V that both $R(r)$ and $R(\nabla)$ give generally the same signs for the rotatory strength with the origin at the CM. However, the problem of choosing the location of the origin, especially in larger molecules, casts doubt on the usefulness of $R(r)$ in calculating rotatory strengths.

D. Sensitivity of Calculated *R* Values. The results obtained here indicate that both the sign and magnitude of the calculated rotatory strength can be affected by configurations which are small contributors to the overall CI wave function. This is due to the coupling of small components with large components in the calculation of R and implies that the complete CI wave function should be employed in the calculation of rotatory strengths.

Acknowledgment. This work was supported by the Division of Chemical Sciences, Office of Basis Energy Sciences of the U. S. Department of Energy. Services and computer time provided by the Argonne National Laboratory Computer Center have been invaluable in this study. We thank Drs. J. D. Petke, S. Peyerimhoff, and R. Buenker for numerous helpful discussions.

Registry No. (*R*)-3-Methylcyclobutene, 20476-28-2.

(43) Brooks, B. R.; Schaefer, H. F., III. *J. Chem. Phys.* **1978**, *68*, 4839–4847.